

Evaluation of laser level populations of erbium-doped glasses

Emerson A. dos Santos^a, Lilia C. Courrol^{a,*}, Luciana R.P. Kassab^a, Laércio Gomes^b,
Niklaus U. Wetter^b, Nilson D. Vieira Jr^b, Sidney J.L. Ribeiro^c, Younes Messaddeq^c

^aLaboratório de Espectroscopia Óptica, FATEC-SP, Praça Coronel Fernando Prestes 30, CEP 01124-060, São Paulo, SP, Brazil

^bCentro de Lasers e Aplicações, IPEN/CNEN-SP, São paulo, SP, Brazil

^cInstituto de Química, UNESP, Araraquara, SP, Brazil

Received 15 February 2005; received in revised form 11 June 2005; accepted 2 March 2006

Available online 19 April 2006

Abstract

A simulation of erbium-doped glass systems, which provides population density for the excited states involved in the 1.5 μm and also for 2.7 μm emissions when pumped around 980 nm, is presented. To describe the diode pump laser processes, a theoretical model based in a coupled system of differential rate equations was developed. The approach used and the obtained spectroscopic parameters are discussed. The materials under study are two oxide glasses, lead fluoroborate ($\text{PbO-PbF}_2\text{-B}_2\text{O}_3$), and heavy metal oxide ($\text{Bi}_2\text{O}_3\text{-PbO-Ga}_2\text{O}_3$) and a fluoride glass ($\text{ZrF}_4\text{-BaF}_2\text{-LaF}_3\text{-AlF}_3\text{-NaF}$), all of them doped with Er^{3+} .

© 2006 Elsevier B.V. All rights reserved.

PACS: 42.70. -a

Keywords: Laser; Glasses; Erbium; Fluorescence

1. Introduction

When choosing a material to be used as an active laser medium, the characteristics desired for good laser performance include, high gain, high-energy storage capacity and low optical losses among others. Gain and energy storage depend on stimulated emission cross-section, fluorescence lifetime, and coupling efficiency with the pump. Solid state Er laser systems pumped by high-power diode lasers have high efficiencies and are now standard tools for many applications [1]. The $^4\text{I}_{13/2} \rightarrow ^4\text{I}_{15/2}$ emission of Er^{3+} at 1.5 μm has been extensively studied for the purpose of developing pulse amplifiers for telecommunication devices made of fiber glasses [2,3]. Telecom wavelength, 1.5 μm for erbium-doped fiber lasers (EDFLs), pumped by solid-state source, make thermal management easier since fibers are long and thin. Sub-picosecond pulse (fs) from passively mode locked fiber laser shown high-energy pulses (nJ) and low cost, comparable to solid state Ti:Sapphire lasers [4].

Also the $^4\text{I}_{11/2} \rightarrow ^4\text{I}_{13/2}$ emission of erbium at 2.7 μm , in fluoride glasses, constitutes a very promising system to build all solid-state lasers emitting near 3 μm to be applied as surgical tools[5,6].

The heavy metal oxides glass ($\text{Bi}_2\text{O}_3\text{-PbO-Ga}_2\text{O}_3$), discovered [7] in 1985, is of great interest in optoelectronic devices due to its properties, namely extended infrared transmission (up to 8 μm), high refractive index (of about 2.5) and nonlinear optical behavior. The literature reports the study of 2.7 and 1.5 μm emissions[8].

Er-doped lead fluoroborate glasses ($\text{PbO-PbF}_2\text{-B}_2\text{O}_3$) have a high refractive index (2.2) that is responsible for the high spontaneous emission probability, very good glass forming region, good physical and chemical stability and transmission from the visible region (0.4 μm) up to the long infrared (4 μm) [9].

Fluoride glasses are well-known for their high transparency in the mid-infrared [10], low phonon energy [11] and low attenuation of radiation near 1.5 μm when comparing with commonly used silica, silicate and phosphate glasses [12]. Particularly the fluorozirconate glasses such as ZBLAN ($\text{ZrF}_4\text{-BaF}_2\text{-LaF}_3\text{-AlF}_3\text{-NaF}$) have unique optical properties in the infrared region [13] and favorable

*Corresponding author. Tel.: +55 111 33222200x2276;
fax: +55 111 3816315.

E-mail address: lcourrol@fatecsp.br (L.C. Courrol).

physical properties [14], which make them excellent candidate materials for optical systems design. Additionally rare earth dopants can be easily introduced into these glasses.

In this paper, the influences of optical parameters of the different erbium doped glasses are calculated by a mathematical model based in the solutions of rate equations of Erbium system.

2. Experiment

The lead fluorborate glasses and heavy metal oxide glasses were produced using, respectively, the glass matrixes $38.8\text{B}_2\text{O}_3\text{--}27.1\text{PbO--}34.1\text{PbF}_2$ and $42.12\text{Bi}_2\text{O}_3\text{--}45.91\text{PbO--}11.98\text{Ga}_2\text{O}_3$. After melting the powders in Pt crucibles at $1000\text{ }^\circ\text{C}$ for 1 h and a half hour, they are poured into heated brass molds ($300\text{ }^\circ\text{C}$), annealed for 3 h at $300\text{ }^\circ\text{C}$ (transition temperature is $380\text{ }^\circ\text{C}$) and then cooled inside the furnace after the furnace is turned off. These oxide glasses were prepared adding Er_2O_3 . ZBLAN glasses were prepared with the following compositions, $53\text{ZrF}_4\text{--}20\text{BaF}_2\text{--}4\text{LaF}_3\text{--}3\text{AlF}_3\text{--}20\text{NaF}$, by melting processing at $750\text{--}800\text{ }^\circ\text{C}$ for 2 h in a tubular furnace. A platinum crucible in the form of a tube was used as a sample container. After fusion, the melt was poured into a stainless steel mold preheated to $260\text{ }^\circ\text{C}$ to form a rectangular glass. Annealing at $260\text{ }^\circ\text{C}$ for 2 h was performed after casting. Finally, the samples were polished using isopropyl alcohol as a lubricating agent. Physical properties of the studied glasses samples are shown in Table 1.

The absorption spectra of all used samples were measured at room temperature in the range $200\text{--}1600\text{ nm}$ using a Varian Spectrometer Cary 17 D. The emission spectra were obtained by exciting the samples, at 965 nm , with a laser diode (Optopower A020). This diode system contains a broad area semiconductor laser with a maximum of 20 W of continuous output power operating at this wavelength. The diode laser beam was conformed to a beam shaper [15] and focused by a single $f = 5\text{ cm}$ lens. Close to the focus, and for a depth of focus of 2 mm , the

beam had a square profile, with transverse dimensions of approximately $260 \times 260\text{ }\mu\text{m}$. During the emission measurements, the samples were pumped with a 7.5 W of diode laser beam, modulated at 40 Hz . The emissions of the samples were analyzed with a 0.5 m monochromator (Spex) and a Germanium detector. The signal was amplified with an EG&G 7220 lock-in and processed by a computer.

A time-resolved luminescence spectroscopy technique was employed to measure the luminescence decays induced by resonant laser excitations, to determine the mechanism involved in the energy transfer up-conversion processes. The excitation system consists of a tunable optical parametric oscillator (OPO from OPOTEK) pumped by the second harmonic of a Q-switched Nd-YAG laser from Quantel. This laser system delivers pulses of 10 mJ with time duration of 4 ns and repetition rate of 10 Hz , and can be tuned from 0.68 to $2.0\text{ }\mu\text{m}$. The time-dependence luminescence of the acceptor was detected by an InSb (77 K) infrared detector (Judson model J10D) with a fast preamplifier (response time of $0.5\text{ }\mu\text{s}$) and analyzed using a signal-processing box-car averager (PAR 4402), or a 200 MHz Tektronix TDS 410 digital oscilloscope. The relative errors in the emission measurements are estimated to be $<5\%$, while errors in the lifetime measurements are $<10\%$.

3. Results

In the three different glass samples we can observe peaks related to the absorption of Er^{3+} around $521, 652, 798, 977$ and 1532 nm arising from the $^4\text{S}_{3/2}, ^4\text{F}_{9/2}, ^4\text{I}_{9/2}, ^4\text{I}_{11/2}$ and $^4\text{I}_{13/2}$ transitions, respectively. The absorption spectra for the three glasses are shown in the Fig. 1. The emissions of the studied glasses around 1.5 and $2.7\text{ }\mu\text{m}$ are shown in Fig. 2.

Let us consider a simplified system represented in Fig. 3. In this system there are two possible up-conversion processes: (1) ESAPR (σ^*): excited state absorption of pump radiation at 976 nm ; (2) ETU (K_i): energy transfer up-conversion by cross relaxation (W_{cr}). The ions are

Table 1
Physical properties of the studied glasses samples

Host	Density (g/cm^3)	Refractive index	Wt%	Er (mol%) (ions/ cm^3)
HMO ($\text{Bi}_2\text{O}_3\text{--PbO--Ga}_2\text{O}_3$)	4.63	2.520	0.68	0.5 (1.74×10^{20})
LF ($\text{PbO--PbF}_2\text{--B}_2\text{O}_3$)	4.40	2.200	0.49	0.5 (1.21×10^{20})
ZBLAN ($\text{ZrF}_4\text{--BaF}_2\text{--LaF}_3\text{--AlF}_3\text{--NaF}$)	5.50	1.498	1.05	2.0 (3.2×10^{20})
HMO	LF			ZBLAN [16]
$\Omega_2 = 1.74 \times 10^{-20}\text{ cm}^2$	$\Omega_2 = 3.51 \times 10^{-20}\text{ cm}^2$			$\Omega_2 = 2.92 \times 10^{-20}\text{ cm}^2$
$\Omega_4 = 0.12 \times 10^{-20}\text{ cm}^2$	$\Omega_4 = 1.09 \times 10^{-20}\text{ cm}^2$			$\Omega_4 = 1.46 \times 10^{-20}\text{ cm}^2$
$\Omega_6 = 0.65 \times 10^{-20}\text{ cm}^2$	$\Omega_6 = 0.94 \times 10^{-20}\text{ cm}^2$			$\Omega_6 = 1.18 \times 10^{-20}\text{ cm}^2$

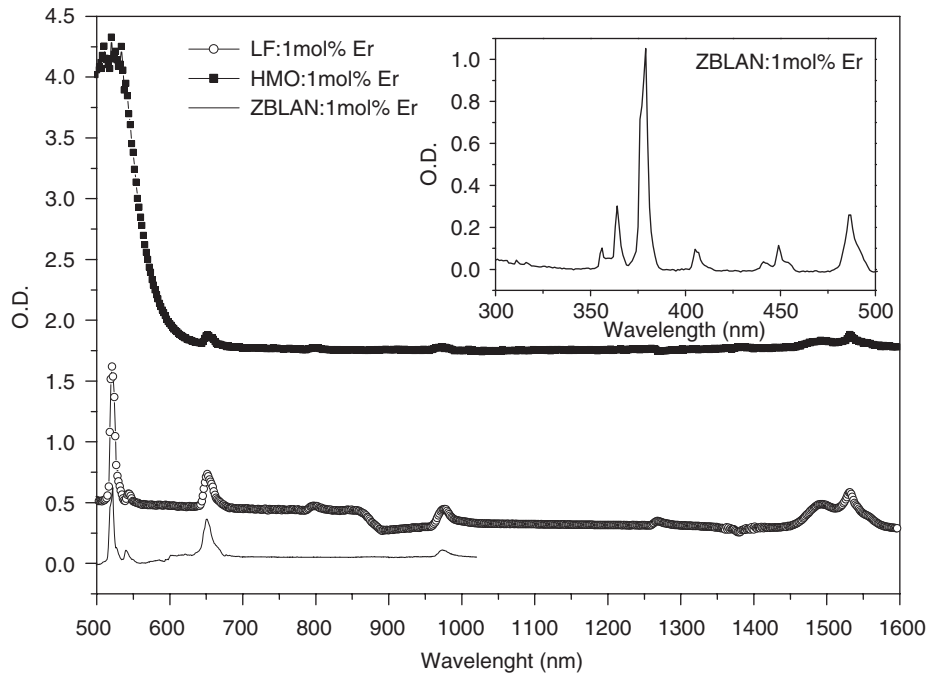


Fig. 1. Absorption spectra for the three studied glasses.

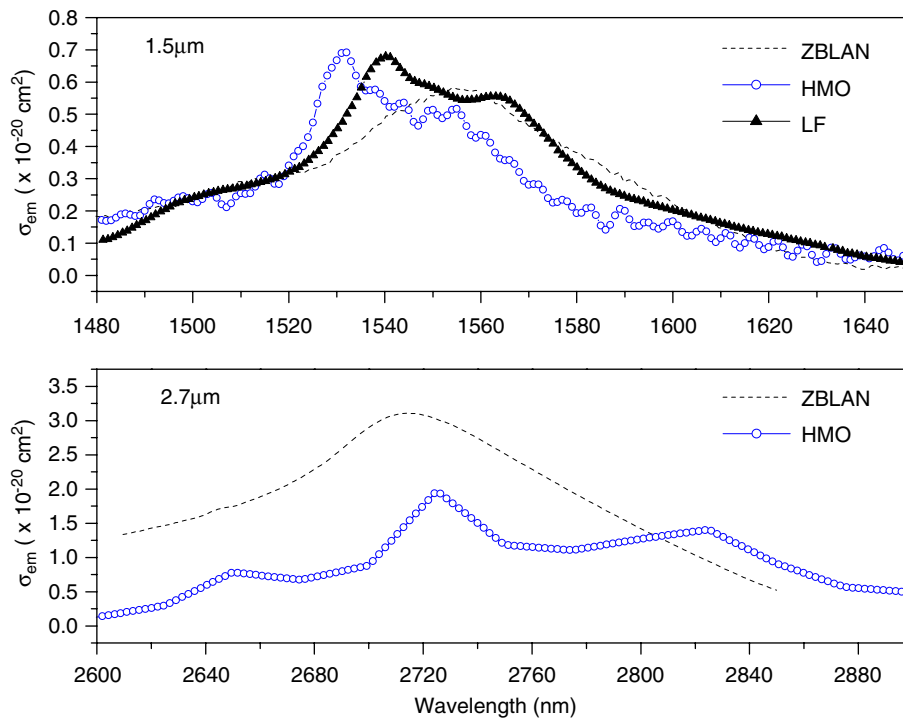
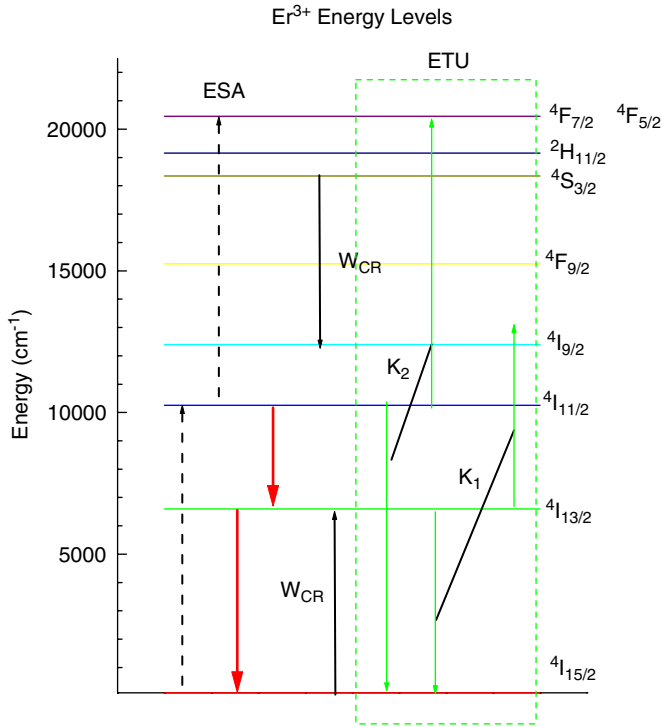


Fig. 2. Emission cross-section spectra of Er^{3+} of the ${}^4\text{I}_{13/2} \rightarrow {}^4\text{I}_{15/2}$ (1.5 μm) and the ${}^4\text{I}_{11/2} \rightarrow {}^4\text{I}_{13/2}$ (2.7 μm) transitions for the studied glasses (excitation at 968 nm).

excited from the ground level 1 (${}^4\text{I}_{15/2}$) to the upper level 3 (${}^4\text{I}_{11/2}$) by the pumping radiation. A second pump photon, or ETU processes, promotes the system to level 4 (the

levels between ${}^4\text{F}_{7/2}$ and ${}^4\text{S}_{3/2}$). The ions in level 3 and 2 (${}^4\text{I}_{13/2}$) can either directly decay to the ground state 1, or to their inferior level or by means of ETU, transferring energy

Fig. 3. Er³⁺ energy levels.

to a neighboring ion, and excite it to level 4. The populations of these levels are then given by

$$\begin{aligned} \frac{dn_1}{dt} &= -n_1 \sigma_a I_p + \frac{n_2}{\tau_2} + \frac{n_3}{\tau_3} + \frac{n_4}{\tau_4} + K_1 n_2^2 + K_2 n_3^2 - W_{CR} n_1 n_4, \\ \frac{dn_2}{dt} &= -\frac{n_2}{\tau_2} - 2K_1 n_2^2 + \beta_{32} \frac{n_3}{\tau_3} + \beta_{42} \frac{n_4}{\tau_4} + W_{CR} n_1 n_4, \\ \frac{dn_3}{dt} &= n_1 \sigma_a I_p - \frac{n_3}{\tau_3} + \beta_{43} \frac{n_4}{\tau_4} - 2K_2 n_3^2 + W_{CR} n_1 n_4 \\ &\quad + K_1 n_2^2 - n_3 \sigma I_p, \\ \frac{dn_4}{dt} &= \frac{n_4}{\tau_4} + K_2 n_3^2 - W_{CR} n_1 n_4 + n_3 \sigma I_p, \\ n_1 + n_2 + n_3 + n_4 &= n_0, \end{aligned} \quad (1)$$

where n_1 , n_2 , n_3 and n_4 are the normalized population of levels 1, 2, 3 and 4, respectively. n_0 is the Er concentration in the glass (given in cm⁻³). σ_a and σ^* are the cross sections of the fundamental and the excited-state absorption of pumping radiation at 976 nm (ESAPR), respectively. I_p is the pumping intensity and τ_2 , τ_3 and τ_4 are the lifetimes of levels 2 (⁴I_{13/2}), 3 (⁴I_{11/2}) and 4 (⁴S_{3/2}). The W_{CR} is the cross relaxation processes from the thermally coupled Er³⁺ ⁴S_{3/2}/²H_{11/2} levels.

At equilibrium, the system must obey the condition:

$$\frac{dn_1}{dt} = \frac{dn_2}{dt} = \frac{dn_3}{dt} = \frac{dn_4}{dt} = 0. \quad (2)$$

The solutions of this system of equation give us directly the population density in function of pumping radiation. To obtain these solutions we need to calculate some of spectroscopic parameters.

ETU parameters were calculated according to a previously published method [16]. In this method, N represents the time-dependent population density of the excited ⁴I_{13/2} level, and then the rate equation for N is given by

$$\frac{dN}{dt} = -\frac{N}{\tau} - 2K_1 N^2, \quad (3)$$

where τ is its intrinsic lifetime, and K_1 is the macroscopic ETU parameter relating to the process (⁴I_{13/2}, ⁴I_{13/2}) → (⁴I_{15/2}, ⁴I_{9/2}). With $N(t=0) = N_0$, integration yields, that is calculated by knowing the absorbed photon density, or the energy absorbed within a pulse, the excited volume determined by the beam waist of laser pumping and the thickness of the sample, and the pump-photon energy. The solution of Eq. (3) is given by

$$N(t) = \frac{N_0 e^{-t/\tau}}{1 + 2K_1 N_0 \tau [1 - e^{-t/\tau}]}. \quad (4)$$

For fitting the first temporal part of the decay when only the directly pumped level is significantly excited and processes involving other excited levels are negligible, especially those processes involving other excited levels, it is possible to obtain the K_1 parameter.

The parameters of ETU from the ⁴I_{13/2} level are evaluated by plotting the data of Fig. 4a by Eq. (4).

The situation is different for the luminescence decay curve and ETU process (⁴I_{11/2}, ⁴I_{11/2}) → (⁴I_{15/2}, ⁴F_{7/2}), from the ⁴I_{11/2} level. ETU from this level populates the ⁴F_{7/2} level from where the excitation relaxes by fast multiphonon decay to the ⁴S_{3/2}/⁴H_{11/2} levels. At a low dopant concentration, these levels decay mostly radiatively to the ⁴I_{15/2} and ⁴I_{13/2} levels and there is no significant back transfer to ⁴I_{11/2} within the time scale relevant for the determination of ETU from ⁴I_{11/2}. At higher dopant concentration, cross relaxation from ⁴S_{3/2}/⁴H_{11/2} levels leads to a fast back transfer into the ⁴I_{11/2} level by multiphonon relaxation. To determine ETU process from ⁴I_{11/2} level, it is necessary to define a branching ratio β , for the part that decay by cross relaxation:

$$\beta = \frac{K_2 n_3 N_0}{n_3 / \tau_3 + K_2 n_3 N_0} = 1 - \frac{\tau_{3\text{eff}}}{\tau_3}. \quad (5)$$

It follows that Eq. (3) changes to:

$$\frac{dN_3}{dt} = -\frac{N_3}{\tau_3} - (2 - \beta) K_2 N_3^2. \quad (6)$$

The K_2 parameters from ⁴I_{11/2} level are evaluated from the data of Fig. 4b by assuming this slope and using the effective lifetimes of ⁴S_{3/2}/⁴H_{11/2} levels and the intrinsic lifetime calculated with Judd Ofelt parameters.

The ETU parameters obtained for ZBLAN glass agree with previous works [16], but divergent values were found for the parameter K_2 for HMO glass [17]. We suppose that this fact is related with the presence of some kind of energy transfer in the glass (for the matrix or oxygen ions) that can produce a decrease in the ⁴I_{11/2} level lifetime and consequently a decrease in the K_2 probability.

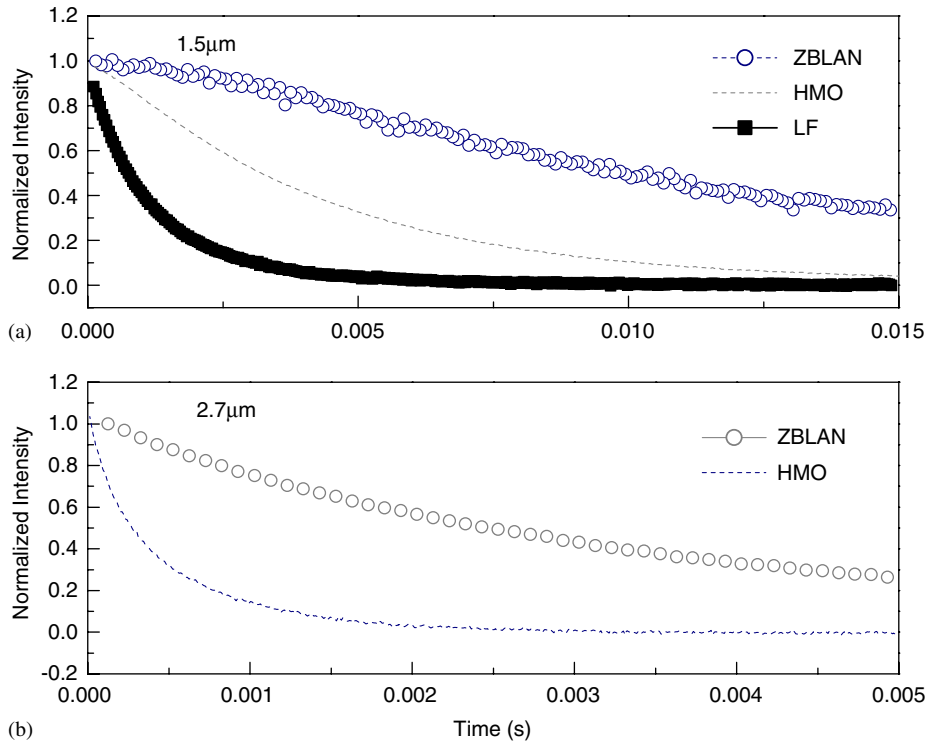


Fig. 4. Measured (and normalized) luminescence-decay curve from the $\text{Er}^{3+} {}^4\text{I}_{13/2}$ level at a wavelength of 1500 nm in the three studied samples (a), and from the ${}^4\text{I}_{11/2}$ level at 2700 nm (b) for ZBLAN and HMO.

The cross relaxation process parameter was obtained from the luminescent decay from the ${}^4\text{S}_{3/2}/{}^2\text{H}_{11/2}$ levels. The rate of W_{CR} process can be described by [16]

$$R_{\text{CR}} = W_{\text{CR}} n_4 n_1,$$

$$1/\tau_{\text{eff}}(n_4) = 1/\tau(n_4) + W_{\text{CR}} N(\text{Er}), \quad (7)$$

where W_{CR} is the macroscopic cross relaxation parameter, n_4 is the population density of the ${}^4\text{S}_{3/2}/{}^2\text{H}_{11/2}$ levels and n_1 is the population density of the ground state considered equal to $N(\text{Er})$, Erbium concentration. The cross relaxation parameters for HMO and ZBLAN are given in the Table 2. The values obtained for ZBLAN agree with results of the literature [16].

The excited state cross-section parameters were calculated from the spontaneous absorption probability from the initial manifold ($S, L, J = 11/2$) to the final manifold ($S', L', J' = 7/2$) determined with the following equation [18]:

$$A_{\text{R}} = \frac{64\pi^4 e^2}{3h(2J+1)\lambda^3} \left(\frac{n(n^2+2)^2}{9} \right) \times \sum_{t=2,4,6} \Omega_t |\langle SLJ || U^t || S'L'J'' \rangle|^2. \quad (8)$$

In equation above, λ is 980 nm. Excited state cross-section for ${}^4\text{F}_{7/2} \rightarrow {}^4\text{I}_{11/2}$ transition is expressed as

$$\sigma_{\text{em}} = \frac{\lambda^4 A_{\text{R}}}{8\pi c \Delta \lambda_{\text{eff}}}, \quad (9)$$

Table 2
Spectroscopic properties of the studied glasses samples

Parameters	HMO	LF	ZBLAN
τ_2 (ms) (${}^4\text{I}_{13/2}$)	3.90	1.10	9.00
τ_3 (ms) (${}^4\text{I}_{11/2}$)	3.80	1.30	6.90
τ_4 (ms) (${}^4\text{S}_{3/2}$)	0.17	—	0.40
β_{43}	0.21	0.22	0.22
β_{42}	0.02	0.02	0.02
β_{32}	0.60	0.59	0.51
K_1 (cm^3/s)	1.3×10^{-17}	1.5×10^{-18}	1.5×10^{-17}
K_2 (cm^3/s)	6.0×10^{-18}	—	0.2×10^{-17}
σ_{ab} (cm^2)	2.6×10^{-21}	8.9×10^{-21}	1.8×10^{-21}
σ^* (cm^2)	1.8×10^{-22}	6.7×10^{-21}	0.5×10^{-21}
σ_{1550} (cm^2)	5.3×10^{-21}	7.3×10^{-21}	5.7×10^{-21}
σ_{2700} (cm^2)	1.9×10^{-20}	—	3.1×10^{-20}
W_{cr} (cm^3/s)	4.8×10^{-18}	—	0.6×10^{-17} [16]

where $\Delta \lambda_{\text{eff}}$ is the effective fluorescence bandwidth. In this case, we considered that the bandwidth is practically the same for the three studied glasses. The obtained values are shown in the Table 2.

Using the measured spectroscopic parameters for the three studied glasses in the solution of rate equations system (1), we obtained the results shown in Table 2 and Fig. 5 for ZBLAN and HMO glasses. LF is not represented in these curves since a non-radiative process leads a high loss in the ${}^4\text{S}_{3/2}/{}^4\text{H}_{11/2}$ population that cannot recycle energy to the ${}^4\text{I}_{13/2}$ level.

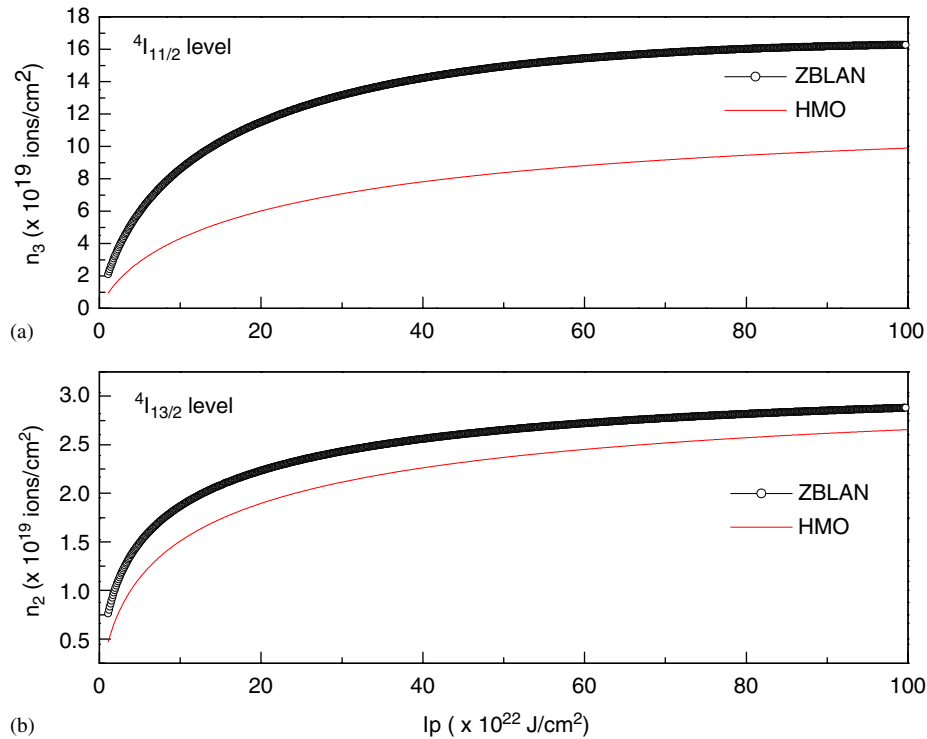


Fig. 5. The population density as a function of pumping radiation; (a) $\text{Er}^{3+} \ ^4\text{I}_{13/2}$, and (b) $\ ^4\text{I}_{11/2}$ level.

For these results we consider that ESA and ETU processes have a fundamental importance in populating the $\ ^4\text{I}_{13/2}$ lower laser level and the $\ ^4\text{I}_{11/2}$ upper laser level.

Observing the Fig. 5, we see that with a pumping intensity of approximately $1.5 \times 10^{23} \text{ J/cm}^2$, the population for the $\ ^4\text{I}_{13/2}$ level is $2.0 \times 10^{19} \text{ ions/cm}^3$ for ZBLAN, and $1.7 \times 10^{19} \text{ ions/cm}^3$ for HMO. For the level $\ ^4\text{I}_{11/2}$ the population density is 2.6×10^{19} for ZBLAN and 1.3×10^{19} for HMO. These results show that both HMO and ZBLAN glasses have very similar properties for $1.5 \mu\text{m}$ laser emission, and can be used for EDFLs configurations. The very wide emission band at $1.5 \mu\text{m}$, for the three studied glasses allows also operation in ultra fast regimes. Considering the $2.7 \mu\text{m}$ laser emission, ZBLAN glass presents better qualities.

4. Conclusions

We have studied the pumping-related up-conversion processes in Er laser glasses. They are significant under typical diode laser pumping intensities, and these processes depend non-linearly on the pumping power. The peak of the excited state absorption cross-section for the pumping radiation at 976 nm , was evaluated to be $0.5 \times 10^{-21} \text{ cm}^2$ (ZBLAN), $1.8 \times 10^{-22} \text{ cm}^2$ (HMO), $6.7 \times 10^{-22} \text{ cm}^2$ (LF). A model to estimate the probability of the ETU process based on $\ ^4\text{I}_{11/2}$ and $\ ^4\text{I}_{13/2}$ levels lifetime curves fit method was utilized, and the ETU parameters were calculated. We found that the values of ETU from the $\ ^4\text{I}_{13/2}$ lower laser level (K_1), which recycles energy to the $\ ^4\text{I}_{11/2}$ upper laser

level, are of the same order of magnitude in HMO and ZBLAN. ETU from the $\ ^4\text{I}_{11/2}$ laser level (K_2), is larger in HMO than in ZBLAN.

By solving the rate equations for the system under continuous pumping, it was possible to estimate the dependence of population density of the $\ ^4\text{I}_{11/2}$ and $\ ^4\text{I}_{13/2}$ levels with the pumping intensity.

The lead fluorborate glass does not produce visible emissions under c.w. diode laser pumping at 976 nm , and losses in the metastable level are observed.

ZBLAN and HMO show emission at $2.7 \mu\text{m}$, but in LF this emission is not observed due to the high phonon energy in this glass. The high phonon energy of the glass host causes large non-radiative decay rates for levels with small energy gaps to the next lower level, and quenches emission from these levels.

Acknowledgments

We would like to thank the support from FAPESP, CNPq, Centro de Lasers e Aplicações, Laboratório de Vidros e Datação da FATEC-SP (Oxide glasses) and Chemistry Faculty of UNESP (Fluoride glass). One of the author (a) thanks FAPESP (no. 03/13614-5) for the fellowship.

References

- [1] W. Lenth, R.M. Macfarlane, Opt. Photon News 3 (1992) 8.
- [2] Y. Miajima, T. Sugawa, Y. Fukasaku, Electron. Lett. 27 (1991) 1706.

- [3] D. Ronarch, M. Guibert, H. Ibrahim, M. Monerie, H. Poignant, A. Tromeur, *Electron. Lett.* 27 (1991) 908.
- [4] H. Endert, et al., *Novel ultrashort pulse fiber lasers for micromachining applications*, Riken Review no. 43, 2002.
- [5] M. Kwasny, Z. Mierczyk, R. Stepien, K. Jedrzejewski, J. Alloys Compounds 300–301 (2000) 341.
- [6] H.M. Percival, D. Szebesta, S.T. Davey, N.A. Swain, T.A. King, *Electron. Lett.* 28 (1992) 2231.
- [7] W.R. Dumbaugh, *Phys. Chem. Glasses* 27 (1986) 119.
- [8] Y.G. Choi, K.H. Kim, *J. Am. Ceram. Soc.* 82 (1999) 2762.
- [9] L.C. Courrol, L.R.P. Kassab, V.D. Del Cacho, S.H. Tatumi, N.U. Wetter, *J. Lumin.* 102 (103C) (2003) 101.
- [10] M.G. Drexhage, in: *Treatise on Materials Science and Technology*, vol. 26, Academic press, Newyork, 1985.
- [11] R. Reisfeld, R. Greenberg, R.N. Brown, M.G. Drexhage, C.K. Jorgensen, *Chem. Phys. Lett.* 95 (1983) 91.
- [12] K. Tanimura, M.D. Shinn, W.A. Silbley, M.G. Drexhage, R.N. Brown, *Phys. Rev. B* 30 (1984) 2429.
- [13] L. Wetenkamp, G.F. West, H. Többen, *J. Non-Cryst. Solids* 140 (1992) 35.
- [14] S.F. Carter, M.W. Moore, D. Szebesta, J.R. Williams, D. Ranson, P.W. France, *Electron. Lett.* 26 (1990) 2116.
- [15] M. Pollnau, P.J. Hardman, W.A. Clarkson, D.C. Hanna, *Opt. Commun.* 147 (1–3) (1998) 203.
- [16] P.S. Golding, S.D. Jackson, T.A. King, M. Pallnau, *Phys. Rev. B* 62 (2) (2000) 856.
- [17] D.J. Coleman, S.D. Jackson, P. Golding, T.A. King, *J. Opt. Soc. Am. B* 19 (2002) 29272936.
- [18] N. Spector, *Chem. Phys. Lett.* 49 (1977) 49.